JOURNAL OF MATERIALS SCIENCE 21 (1986) 4188–4192

The effect of phase segregation during structural relaxation of $Fe_{10}Ni_{65}Si_{10}B_{15}$ spin glass in the amorphous state

A. J. JANICKI, C. A. FAUNCE, R. S. TEBBLE
Department of Pure and Applied Physics, University of Salford, Salford M5 4WT, UK

The structural relaxation process of $Fe_{10}Ni_{65}B_{15}Si_{10}$ amorphous spin glass is described. The ribbon samples were prepared by melt spinning and heat treated using two different annealing processes: AP1 and AP2. The techniques employed to investigate structural changes in the three alloy states as-quenched (AQ), AP1 and AP2 were as follows: transmission electron microscopy, scanning electron microscopy with X-ray analysis, differential scanning calorimetry. Differences were detected in the amorphous structures for two states of relaxation in the alloy. The formation of clusters is proposed for one alloy state and the influence of clustering on the early stages of crystallization is discussed.

1. Introduction

During recent years many papers have been published dealing with spin glasses; however, most of them are primarily concerned with magnetic properties and the nature of the origin of boundary lines around the multicritical point (MCP). The magnetic properties of spin glass alloys are strongly dependent on the location of atoms in the amorphous structure, and invariably spin glass models are based on the assumption of an exchange interaction between a given atom and its near-neighbours [1–7]. Therefore, it follows that variations in atomic positions in the amorphous state incurred during structural relaxation will have a considerable effect on the exchange interaction and, of course, the magnetic nature of the spin glass. The subject of this investigation is the amorphous alloy $Fe_{10}Ni_{65}B_{15}Si_{10}$.

2. Experimental details

A metallic glass ribbon $Fe_{10}Ni_{65}B_{15}Si_{10}$, 8 mm wide and 30 μm thick was produced by the melt spinning technique.

The amorphous state of the ribbon was established by X-ray diffraction using Cu$K\alpha$ radiation. The ribbon samples were heat-treated in quartz ampoules under high vacuum, using two different annealing processes:

AP1: the ribbon annealed at 570 K for 25 h (i.e. $T_x|20\,\mathrm{K\,min^{-1}}| - 150\,\mathrm{K}$).

AP2: as for AP1 samples plus 620 K for 75 h (i.e. $T_x|20\,\mathrm{K\,min^{-1}}| - 100\,\mathrm{K}$).

The amorphous state was reconfirmed after each of the above treatments.

Thin foil microscope specimens were prepared using a Struers double side thinning apparatus, and a Jeol 200CX transmission electron microscope (TEM) was used to study morphology and the first stages of crystallization. The same techniques were used to prepare and examine both thin foil and bulk ribbon specimens.

A differential scanning calorimeter (DSC) DuPont 910/990 was employed to determine the onset of the crystallization temperature, T_x, and the activation energy for crystallization, E_a, which was calculated by the Kissinger method.

Flat, 0.25 μm diamond polished cross sections of AQ, AP1 and AP2 samples were examined and analysed using a Cambridge 604 scanning electron microscope (SEM) with a Link X-ray energy dispersive analyser.

3. Results

The X-ray diffraction pattern of AQ $Fe_{10}Ni_{65}B_{15}Si_{10}$ exhibits an amorphous structure over the entire ribbon, with an average d space of 0.198 nm.

3.1. DSC measurements

A typical thermogram at a heating rate of 20 K min^{-1} is shown in Fig. 1. The values of crystallization temperature (T_x) and activation energy (E_a) for AQ, AP1 and AP2 materials are listed in Table I. The effect of the first annealing process AP1 is to increase the T_{x1} temperatures, which may be clearly seen from results of the lower heating rates; however, there is no noticeable change in the values of the T_{x2} temperatures. The second annealing process AP2 produces very little change in the value of the T_{x1} temperature and causes a slight decrease in the value of the T_{x2}.

The activation energy of the first stages of crystallization, E_{a1} increased gradually for both AP1 and AP2 processes, while E_{a2} remained unchanged. Further experiments were carried out on the SEM and TEM to investigate the rise in E_{a1} more closely.

3.2. TEM

The *in situ* early stages of crystallization were observed using a heating holder in the TEM and the estimated

0022–2461/86 $03.00 + .12

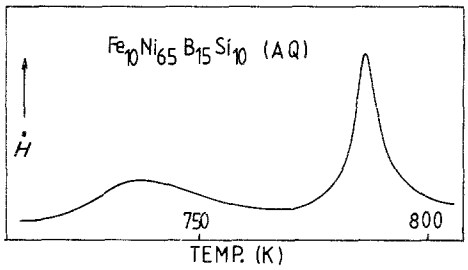

Figure 1 DSC thermogram at heating rate 20 K min^{-1}.

average heating rate was 10 K min^{-1}. Figs 2 and 3 present crystallization sequences of AP1 and AP2 samples, respectively.

AP1 spin glass crystallized in four stages, as follows:

I. 300 to 520 K, the d spacing of the amorphous phase (d_{AM}) remains unchanged at 0.2075 nm.

Ia. 520 to 670 K, the value of d_{AM} increases to 0.2098 nm; however the alloy remains in the fully amorphous state (Fig. 2a).

II. 670 to 730 K, first crystals of spherulitical morphology appear, and the d_{AM} value remains as in stage Ia despite an increase in the degree of crystallinity and a rise in temperature (Figs 2b, c).

III. Annealing at 730 K for 15 min, results in a further increase in both crystal size and number, d_{AM} increases slightly to 0.2125 nm (Figs 2d, e), further annealing for 20 min results in total decomposition of amorphous phase.

The crystallization of AP2 material proceeded as follows:

I. 300 to 680 K, alloys remain fully amorphous with d_{AM} = 0.211 nm (Fig. 3a).

II. 680 to 740 K, microcrystals appear in large number and as crystallization progresses d_{AM} increases to 0.215 nm (Fig. 3b).

III. 740 K, a fully decomposed amorphous phase, and a microcrystalline structure with polygonal morphology (Figs 3c, d).

The following differences in the crystallization between AP1 and AP2 specimens were observed:

1. d_{AM} of AP2 material does not change until the onset of the crystallization, i.e. 680 K, but the d_{AM} of AP1 material starts to increase at 520 K, when the alloy is still fully amorphous.

2. The nucleation rate of the AP2 material is much higher than that of the AP1.

3. In stage II, after the onset of crystallization d_{AM} remains constant for AP1 and changes for AP2 material.

Heating experiments on bulk ribbon specimens of (AP1) and (AP2) treated material were also carried out and TEM observations made on these samples exhibited the same changes in structure and morphology as for corresponding thin foil specimens.

3.3. SEM with X-ray energy dispersive analysis

The cross-section of AQ, AP1 and AP2 ribbons has been analysed for variation in iron and silicon content. No variations in composition were encountered over a large number of spot analyses for either AQ or AP1 ribbon; however, this was not the case for AP2. On the basis of analyses of several different lengths of ribbon calculations confirm that:

1. the iron content for AP2 material showed a $\pm$ 10% variation from the average value obtained for the sample;

2. the silicon content varied about $\pm$ 16% from the average value for AP2 material;

3. when the results obtained for AQ and AP1 materials were compared no significant differences in composition were detected for iron or silicon.

4. Discussion

Specimens subjected to the first annealing process (AP1) exhibited an increase in thermal stability, i.e. an increase of 10% in E_a, and a marginal increase in T_x, which is particularly noticeable at the lower heating rates. The crystallization mechanism, nucleation rate and the morphology of the first crystals to appear remain unchanged for both AQ and AP1 materials. Results from the SEM confirm the similarity of AQ and AP1 materials with respect to local variations in composition. Relaxation, according to Graham and Egami [8], is characterized by the elimination of excess free volume and either the annihilation or transformation of large unstable defects to smaller more stable defects. Results obtained from AP1 specimens show a constant value of d_{AM} up to a temperature of 520 K followed by an increase in this parameter to a temperature of 670 K. This indicates there is a thermal activation threshold for the transformation to smaller but more stable defects. It is therefore likely that the first stage of relaxation was attained during the process AP1. Because of the higher temperature inherent in the AP2 annealing process, there is no observed change in the value of d_{AM} suggesting that the defect transformation has been completed. On the basis of the SEM results (Section 3.3) it would appear that in the early stages of crystallization of the AP2 samples, a phase segregation process takes place. This segregation process is considered to be characterized by a regrouping of iron and metalloid atoms and results both in a breakdown in homogeneity and the

TABLE I T_x, E_a for $Fe_{10}Ni_{65}B_{15}Si_{10}$ in AQ, AP1 and AP2 state

	Heating rate (K min^{-1})					E_{a1} (eV)	E_{a2} (eV)
	5	10	20	50	100		
	T_{x1}, T_{x2} (K)	T_{x1}, T_{x2} (K)	T_{x1}, T_{x2} (K)	T_{x1}, T_{x2} (K)	T_{x1}, T_{x2} (K)		
AQ	704, 763	715, 775	721, 782	737, 795	744, 800	3.25	4.68
AP1	706, 763	716, 775	722, 780	739, 797	744, 800	3.55	4.62
AP2	707, 762	717, 775	723, 780	738, 794	743, 800	3.87	4.68

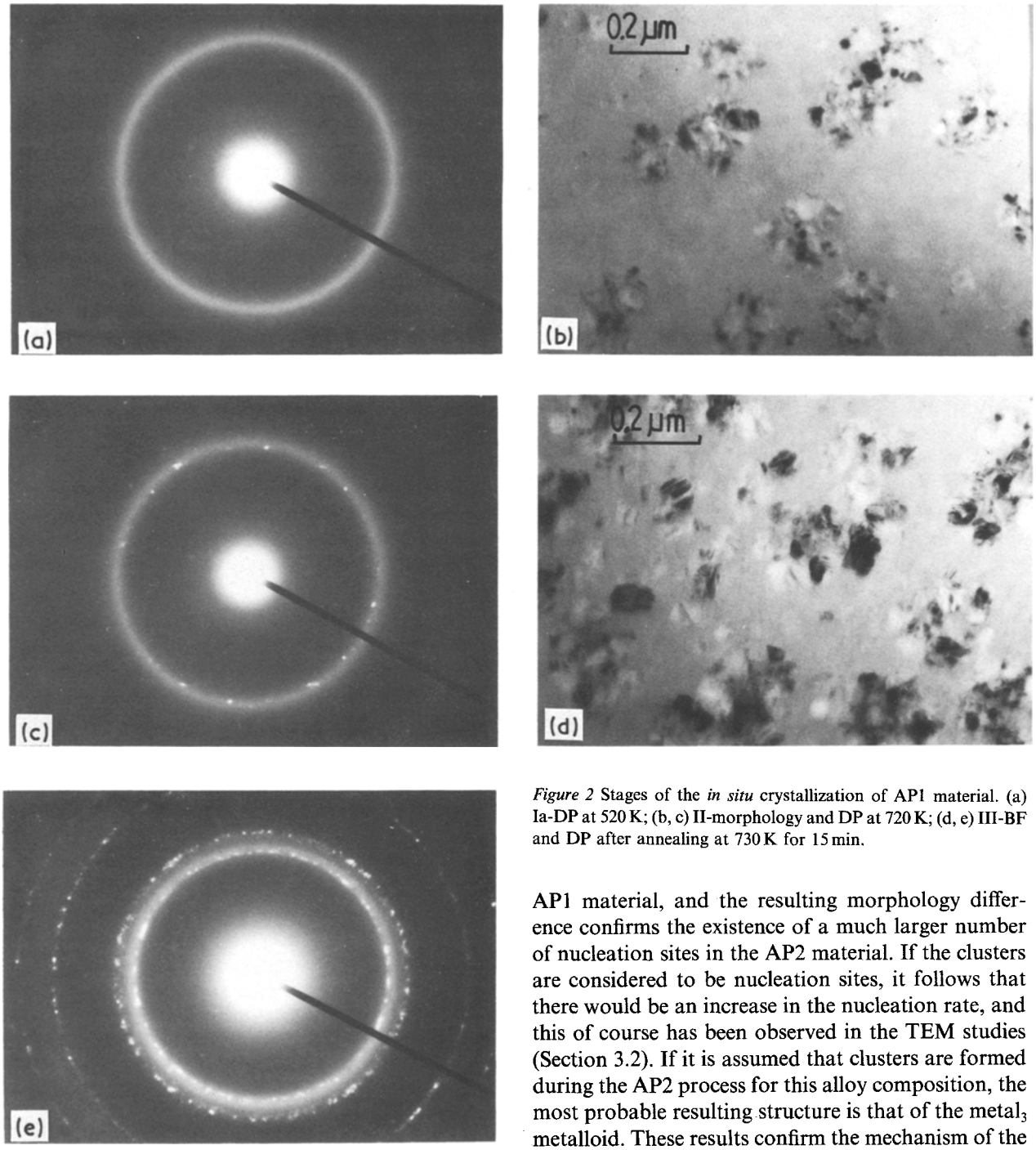

Figure 2 Stages of the *in situ* crystallization of AP1 material. (a) Ia-DP at 520 K; (b, c) II-morphology and DP at 720 K; (d, e) III-BF and DP after annealing at 730 K for 15 min.

formation of areas of high iron and metalloid atom concentrations. Furthermore, the probability of an increase in Fe–Fe pair concentration is likely and this would obviously affect the magnetic properties at low temperature. The structure still remains fully amorphous however, and shows higher thermal stability exhibited by the fact that the value of d_{AM} remains unchanged until 680 K. That higher thermal stability results from the AP2 annealing process is further confirmed by the increase in E_{a1} and T_{x1} as shown in Section 3.1. This is indicative of a regrouping of atoms to form clusters to produce a more favourable energy condition within the alloy.

$Metal_3$ metalloid clusters in the amorphous phase were proposed by Pillar and Haasen [9] and applied by Zielinski and Ast [10] to an interpretation of the relaxation mechanism for $(Fe, Ni)_{80}(B, Si)_{20}$ alloys. The nucleation rate for AP2 is much higher than for the AP1 material, and the resulting morphology difference confirms the existence of a much larger number of nucleation sites in the AP2 material. If the clusters are considered to be nucleation sites, it follows that there would be an increase in the nucleation rate, and this of course has been observed in the TEM studies (Section 3.2). If it is assumed that clusters are formed during the AP2 process for this alloy composition, the most probable resulting structure is that of the $metal_3$ metalloid. These results confirm the mechanism of the two stage relaxation process proposed by Van den Beukel and Radelaar [11], which suggests the annihilation of excess free volume in the first stage and the regrouping of atoms in short-range order (SRO) in the second stage of relaxation.

A number of papers have appeared reporting metal–metalloid bonding interaction for most metal–metalloid multicomponent glasses [12–14]. When the results of these works were fitted to those of the alloy used in this investigation the most probable structure of the clusters in the AP2 material was found to be Ni_3B, although $FeNi_2B$ cannot be completely excluded. To support this finding, electron diffraction patterns were measured and these results confirmed that the first crystals to appear correspond to the Ni_3B phase. It would, therefore, appear that these crystals have developed from clusters of a similar structure and composition. The formation of such clusters is further substantiated by the results of Vincze *et al.* [15] and

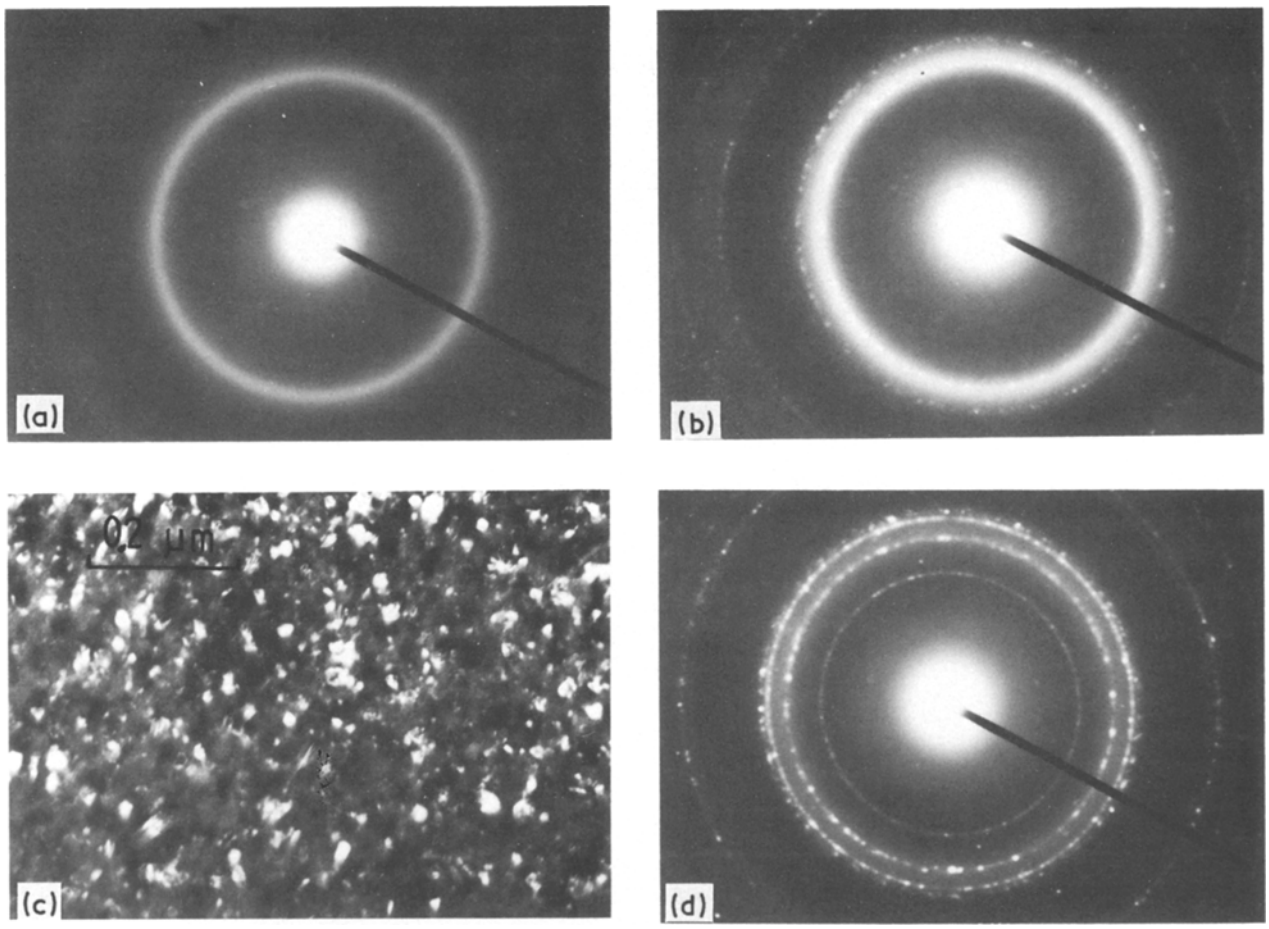

Figure 3 Stages of the *in situ* crystallization of AP2 material; (a) I-DP at 680 K; (b) II-DP at 730 K; (c, d) III-morphology DF and DP at 740 K.

Walter [16], where it has been shown that preferential bonding takes place between nickel and boron atoms.

In the investigation of spin glasses by Crook *et al.* [17] it was pointed out that the spin glass temperature, T_f, and the Curie temperature, T_c, are both functions of the density of the magnetic atoms. Tentative measurements of susceptibility have been carried out on $Fe_{10}Ni_{65}B_{15}Si_{10}$ ribbon (not reported in this paper), and the results show that the annealing process has a definite effect on this parameter: that is, the T_f temperature remains constant within experimental limits for materials AQ and AP1 and there is a slight increase in the value for AP2. It therefore seems reasonable to assume that the spin glass transformation also depends on the particular positions taken up by the magnetic atoms, i.e. on the relaxation state of the alloy.

5. Conclusion

The object of this research was to exhibit how annealing and the resulting relaxation, affects the amorphous structure of spin glass, after two different heat treatments.

Experimentally, two annealing temperatures and times were chosen to produce two different types of amorphous structures. Clustering resulting in phase segregation is described, as well as its effect on the early stages of the crystallization process.

The results of this work should be useful in explaining the changes in magnetic properties, transition temperature, T_f, and Curie temperature, T_c, for various relaxation states in spin glass.

Acknowledgement

The research was sponsored by USAF Grant No. AFOSR-80-0005 and this support is gratefully acknowledged.

References

1. P. A. BECK, in "Magnetism in Alloys" (ISM–AIME, New York, 1972).
2. J. L. THOLENCE and R. TOURNIER, *J. Phys. Colloq.* **35** (1974) 229.
3. I. REISS, *Commun. Phys.* **2** (1977) 37.
4. U. LARSEN, *Phys. Rev. B* **14** (1976) 4356.
5. S. F. EDWARDS and P. W. ANDERSON, *J. Phys. F* **5** (1976) 965.
6. D. SHERRINGTON and S. KIRKPATRICK, *Phys. Rev. Lett.* **35** (1975) 1792.
7. C. M. SOUKOULIS and K. LEVIN, *Phys. Rev. B* **18** (1978) 1439.
8. C. D. GRAHAM and T. EGAMI, *Ann. Rev. Mater. Sci.* **8** (1978) 423.
9. J. PILLER and P. HAASEN, *Acta Metall.* **30** (1982) 1.
10. P. G. ZIELINSKI and D. G. AST, *J. Non-Cryst. Solids* **61/62** (1984) 1021.
11. A. VAN DEN BEUKEL and S. RADELAAR, *Acta Metall.* **31** (1983) 419.
12. H. S. CHEN, *ibid.* **22** (1974) 897.
13. W. I. JOHNSON and A. R. WILLIAMS, *Phys. Rev. B* **20** (1979) 1640.

14. R. P. MESSMER, *ibid.* **23** (1981) 1616.
15. I. VINCZE, D. S. BOUDREAUX and M. TEGZE, *Phys. Rev. B* **19** (1979) 4896.
16. J. L. WALTER, *J. Mater. Sci. Eng.* **39** (1979) 95.
17. R. CROOK, E. D. DAHLBERG and K. V. RAO, Proceedings of the 5th Rapidly Quenched Metals Conference, edited by S. Steeb and H. Warlimont, Wuerzburg (1984) paper G33 (Elsevier, 1985) p. 1239.

Received 21 October 1985
and accepted 11 February 1986